Macromolecules
ARTICLE

Macromolecules **2010**, *43*, 10397–10405 **10397**
DOI: 10.1021/ma101180k

High Modulus, Low Surface Energy, Photochemically Cured Materials from Liquid Precursors

Zhaokang Hu,[†] Louis M. Pitet,[§] Marc A. Hillmyer,[§] and Joseph M. DeSimone*[,†,‡]

[†]*Department of Chemistry, University of North Carolina at Chapel Hill, Chapel Hill, North Carolina 27599, United States,* [‡]*Department of Chemical Engineering, North Carolina State University, Raleigh, North Carolina 27695, United States, and* [§]*Department of Chemistry, University of Minnesota, Minneapolis, Minnesota 55455, United States*

Received May 27, 2010; Revised Manuscript Received October 25, 2010

ABSTRACT: A new strategy has been developed to achieve durable, low surface tension fluorinated polymeric materials by copolymerizing a tetramethacryloxy-modified perfluoropolyether (PFPE) macromonomer and a fluorinated difunctional cross-linker, 1*H*,1*H*,6*H*,6*H*-perfluoro-1,6-hexyl diacrylate (PFHDA), into very highly cross-linked materials that possess a very high modulus as well as a very low surface energy. The miscibility of the two fluorinated components has been studied by measuring the cloud-point temperatures. Partially miscible mixtures yielded optically transparent samples after curing at low PFHDA contents (e.g., < 40 wt %), and cloudy samples were obtained at high PFHDA contents when cured at room temperature. However, it was possible to achieve optically transparent samples with high PFHDA contents by increasing the cure temperature. The miscibility of these materials has been further studied by differential scanning calorimetry (DSC), dynamic mechanical thermal analysis (DMTA), and atomic force microscopy (AFM). By incorporating PFHDA into the cross-linked system, a low surface energy, very high modulus (up to 458 MPa) thermoset could be achieved which is important for many applications including as hard, abrasion-resistant coating materials.

Introduction

There are significant needs for high modulus, durable, low surface energy materials for a range of applications including for use in medical devices, molding materials for imprint lithography and environmentally friendly marine fouling-release coatings. For example, silicone rubber has been considered for numerous long in-dwelling medical device applications but can be hampered by the significant adsorption and absorption of lipids during deployment due to the high solubility of oleophilic materials in silicones.[1] In imprint lithography, high modulus forms of poly(dimethylsiloxane) (PDMS), referred to as hPDMS, have been developed to achieve high-performance properties in molding and printing applications.[2] Fluoropolymer alternatives to silicones have also been developed to lower the surface tension and to further decrease the permeability of organics into such molding materials. In particular, perfluoropolyethers have been developed as alternatives to silicones for use in microfluidics and imprint lithography.[3−6]

Nontoxic polymeric fouling-release coatings are environmentally friendly alternatives to toxic, antifouling coatings. According to Baier and Brady's research, polymeric materials with low surface tension and low modulus were apt to provide surfaces with low adhesion forces to attached fouling species.[7,8] Though the mechanisms of controlling fouling-release behavior are not fully understood,[9] the low surface tension and modulus design criteria have been widely accepted in the biofouling community since this observation has been supported by numerous related studies.[10−15] The low surface tension of nonpolar materials was thought to reduce ionic and polar chemical interactions between adhesives and coatings,[16] while having a low modulus served to minimize mechanical locking and facilitates the breaking of adhesive joints.[17,18] Therefore, polymeric materials combining these two factors are favored as promising candidates for fouling-release applications. One example is PDMS, which possesses a low surface tension of ∼25 mN/m and low modulus (2.4 MPa for fully cured Sylgard 184).[7,19−21] With even lower surface tensions compared to PDMS, fluorinated polymers have recently drawn attention as fouling-release coating materials.[22,23] Additionally, fluorinated polymers exhibit exceptionally high chemical and thermal stabilities imparted by the strong C−F and C−C bonds,[24] which prevents swelling and loss of mass caused by degradation upon long-term water exposure.

Previously studied perfluoropolyether (PFPE) elastomeric materials were photochemically cross-linked from a series of difunctional macromonomers with various end groups and molar masses.[25] These PFPE materials exhibited low surface tensions and high flexibility. However, the highest Young's modulus achieved was only 90 MPa for a dimethacryloxy-modified PFPE material (M_n = 1 kg/mol). A higher Young's modulus is thought to be necessary to achieve better durability for a long-term fouling-release coating application.[26] As such, it is of practical importance to develop strategies that increase the modulus, while maintaining the low surface tension of the current photochemically cross-linked systems. According to the literature, various inorganic nanoparticles such as titanium oxide, silica, and carbon nanotubes were widely used as reinforcing fillers to increase the modulus of cross-linked systems.[27−29] However, while the addition of nanoparticles worked well for many hydrocarbon-based polymers, the high interfacial energy between perfluorinated polymer matrices with inorganic nanoparticles made homogeneous dispersion difficult. An alternative to avoid possible immiscibility issues associated with inorganic nanoparticles is to incorporate difunctional organic small molecules into cross-linked matrices.[30] Organic compounds can dissolve and

*To whom correspondence should be addressed: e-mail desimone@unc.edu.

Published on Web 11/19/2010

mix well in prepolymer systems and can form highly cross-linked hard materials. Additionally, multifunctional macromonomers with large functionalities (i.e., $f > 2$) can be synthesized and copolymerized with difunctional cross-linkers to generate densely cross-linked networks upon curing.[31]

In this paper, a commercially available perfluoropolyether tetrol oligomer was modified to form a tetramethacryloxy-functionalized perfluoropolyether (PFPETMA) macromonomer with functionality (f) equal to eight (in chain growth chemistry a vinyl group has a functionality, f, equal to two so a tetramethacryloxy-functionalized macromonomer has $f = 8$). This macromonomer was then photochemically cross-linked to form a hard fluorinated network. Meanwhile, a short chain cross-linker, 1*H*,1*H*,6*H*,6*H*-perfluoro-1,6-hexyl diacrylate (PFHDA), was copolymerized with the PFPETMA macromonomer to further increase the modulus upon curing. One advantage of the PFHDA additive is that the perfluorinated molecule appeared to be miscible with the PFPETMA macromolecule matrix to yield a homogeneous solution at room or at moderately elevated temperatures. The liquid binary system was then photochemically cross-linked using UV light to form optically transparent films. Phase separation and morphologies of these cured samples were studied by a variety of techniques including differential scanning calorimetry (DSC), dynamic mechanical thermal analysis (DMTA), small-angle X-ray scattering (SAXS), and atomic force microscopy (AFM). This study helped to elucidate the miscibility and compatibility behavior between the two fluorinated components and optimize the design of perfluorinated systems to obtain durable materials as long-term fouling-release coating materials.

Experimental Section

Materials. The solvent 1,1,1,3,3-pentafluorobutane (Solkane 365 MFC) was purchased from Micro-Care. The 1*H*,1*H*,6*H*,6*H*-perfluoro-1,6-hexyl diacrylate (PFHDA) additive was purchased from Oakwood Products, Inc. The Fomblin Z03 (M_n = 4 kg/mol) was purchased from Solvay Solexis. Poly(tetrafluoroethylene oxide-*co*-difluoromethylene oxide) α,ω-bis(2,3-dihydroxypropyl-ether) (PFPE tetrol, M_n = 2 kg/mol), tetrabutyltin diacetate (DBTDA), α-hydroxycyclohexyl phenyl ketone (HCPK), and 2-isocyanatoethyl methacrylate (IEM) were purchased from Sigma-Aldrich. All of the chemicals were used as received.

Synthesis of Tetramethacryloxy-Modified Perfluoropolyether Macromonomer (PFPETMA). The tetramethacryloxy-modified perfluoropolyether (PFPETMA) macromonomer was synthesized by the following procedure. In a typical synthesis, 10 g of the PFPE tetrol (5 mmol) was added to 50 mL of 1,1,1,3,3-pentafluorobutane to form a slightly cloudy liquid mixture, which was followed by the addition of 3.1 g of 2-isocyanatoethyl methacrylate (IEM, 20 mmol) and 0.1 mL of tetrabutyltin diacetate (DBTDA) as a catalyst. The solution was kept under a nitrogen flow, and upon mild stirring and heating to 45 °C, the initially turbid solution became clear after ~5 min. After 8 h, the reaction solution was passed through a chromatographic column filled with alumina (2 × 10 cm) followed by evaporation of the solvent to yield a clear, colorless, viscous oil. ^{1}H NMR (400 MHz, $CDCl_3$): δ [ppm] = 1.94 (s, CH_3), 3.50 (m_c, $NHCH_2CH_2O$), 3.75 (m_c, $OCH_2CH(O)CH_2O$), 3.87 (m, CF_2CH_2O), 4.22 (m, $NHCH_2CH_2O$), 4.30 (m, $OCH_2CH(O)CH_2O$), 5.09 (bs, N*H*), 5.59 and 6.11 (s, $C{=}CH_2$). FTIR: ν = 3340, 2960, 1720, 1638, 1540, 1450, 1398, 1055−1200, 941, 811, and 680 cm^{-1}.

Photocuring of PFHDA−PFPETMA Samples. The clear, solvent-free PFPETMA precursor with 0.2 wt % of α-hydroxycyclohexyl phenyl ketone (HCPK) photoinitiator added was cast on a clean silicon wafer and then photochemically cured to form an optically transparent cross-linked elastomeric film via UV irradiation (Electronlite UV curing chamber model no. 81432-ELC-500, λ = 365 nm) under nitrogen purge for 5 min (~38 000 mJ/cm^2). The poly(perfluorohexyl diacrylate-*co*-tetramethacryloxy perfluoropolyether) (p(PFHDA−PFPETMA)) elastomeric network material was obtained by photochemically cross-linking the liquid binary system consisting of the PFPETMA macromonomer and 1*H*,1*H*,6*H*,6*H*-perfluoro-1,6-hexyl diacrylate (PFHDA) in a desired weight composition ratio in a similar manner. Because of the partial immiscibility of the two components, while the cross-linked p($PFHDA_{0.2}$−$PFPETMA_{0.8}$) and p($PFHDA_{0.4}$−$PFPETMA_{0.6}$) samples were optically transparent, the p($PFHDA_{0.6}$−$PFPETMA_{0.4}$) and p($PFHDA_{0.8}$−$PFPETMA_{0.2}$) samples were cloudy upon UV curing at room temperature. However, optically transparent samples of p($PFHDA_{0.6}$−$PFPETMA_{0.4}$) and p($PFHDA_{0.8}$−$PFPETMA_{0.2}$) could be obtained by heating the samples during curing. To do this, a heating plate with a precisely controlled temperature was placed inside the UV chamber, and a piece of silicon wafer was put atop the heating plate followed by pouring the cloudy liquid mixture onto the silicon wafer. Heating the system to a temperature slightly higher than the cloud point, i.e., 65 °C for p($PFHDA_{0.6}$−$PFPETMA_{0.4}$) and 85 °C for p($PFHDA_{0.8}$−$PFPETMA_{0.2}$), the cloudy mixture turned to an optically clear homogeneous solution. The solution was then cross-linked by UV curing. Both the cured p($PFHDA_{0.6}$−$PFPETMA_{0.4}$) and p($PFHDA_{0.8}$−$PFPETMA_{0.2}$) samples were optically transparent that were obtained in this manner and remained so even after cooling to room temperature.

Characterization. Nuclear magnetic resonance (NMR) spectra were taken using a Bruker 400 MHz DRX spectrometer. Fourier transform infrared spectrometry (FTIR) was obtained with a Tensor 27 FTIR instrument (Bruker) with a 4 cm^{-1} resolution and 32 scans. Atomic force microscopy (AFM) was obtained with an Asylum MFP-3D scanning probe microscope at ambient conditions using Tap300Al-G (tapping mode) cantilevers (Budget Sensors). The AFM phase contrast images were taken on the cross section of samples cut by a Reichert Supernova ultramicrotome. Small-angle X-ray scattering (SAXS) measurements were acquired at Beamline 5-ID at the Advanced Photon Source (APS) at Argonne National Laboratories, maintained by the Dow−Northwestern−Dupont Collaborative Access Team (DND-CAT). The samples were 0.2−0.3 mm in thickness. The source produces X-rays with a wavelength (λ) of 0.729 Å at a sample-to-detector distance of 5.6 m calibrated with silver behenate. Scattering intensity was monitored by a Mar 165 mm diameter CCD area detector. Differential scanning calorimetric (DSC) measurements were conducted using a Seiko DSC 220. The samples were first heated to 150 °C and then cooled to −150 °C at a rate of 80 °C/min. Thermographs were then recorded from −150 to 120 °C at a heating rate of 10 °C/min. Dynamic mechanical thermal analysis (DMTA) measurements were performed in a PerkinElmer Pyris Diamond DMA 6100, operating at a fixed frequency (1 Hz) in tension mode. The temperature was varied from −150 to 150 °C with a heating rate of 2 °C/min. The cloud-point temperature curve of the PFHDA−PFPETMA binary system was determined by cooling the liquid mixture of a known composition ratio from 120 °C in a temperature-controlled oil bath to the temperature where the clear liquid solution was observed to become cloudy. Stress−strain measurements were performed on rectangular samples (1 × 10 × 15 mm) at room temperature on an Instron model 5566 system using a 10 kN load cell at a crosshead speed of 5 mm/min. An extensometer of 15 mm gauge length was used to measure the strain accurately. The static sessile drop contact angles of water and *n*-hexadecane on the surfaces were measured using a KSV Instruments LCD CAM 200 optical contact angle meter at room temperature (23 °C).

Results and Discussion

The PFPE tetrol oligomer (M_n = 2 kg/mol) was partially soluble in 1,1,1,3,3-pentafluorobutane, resulting in a slightly optically cloudy mixture at room temperature. With dibutyltin diacetate (DBTDA) as a catalyst, isocyanatoethyl methacrylate quickly reacted with the hydroxyl end groups of the

Scheme 1. Synthesis of PFPETMA Macromonomer and Its Cross-Linking with PFHDA

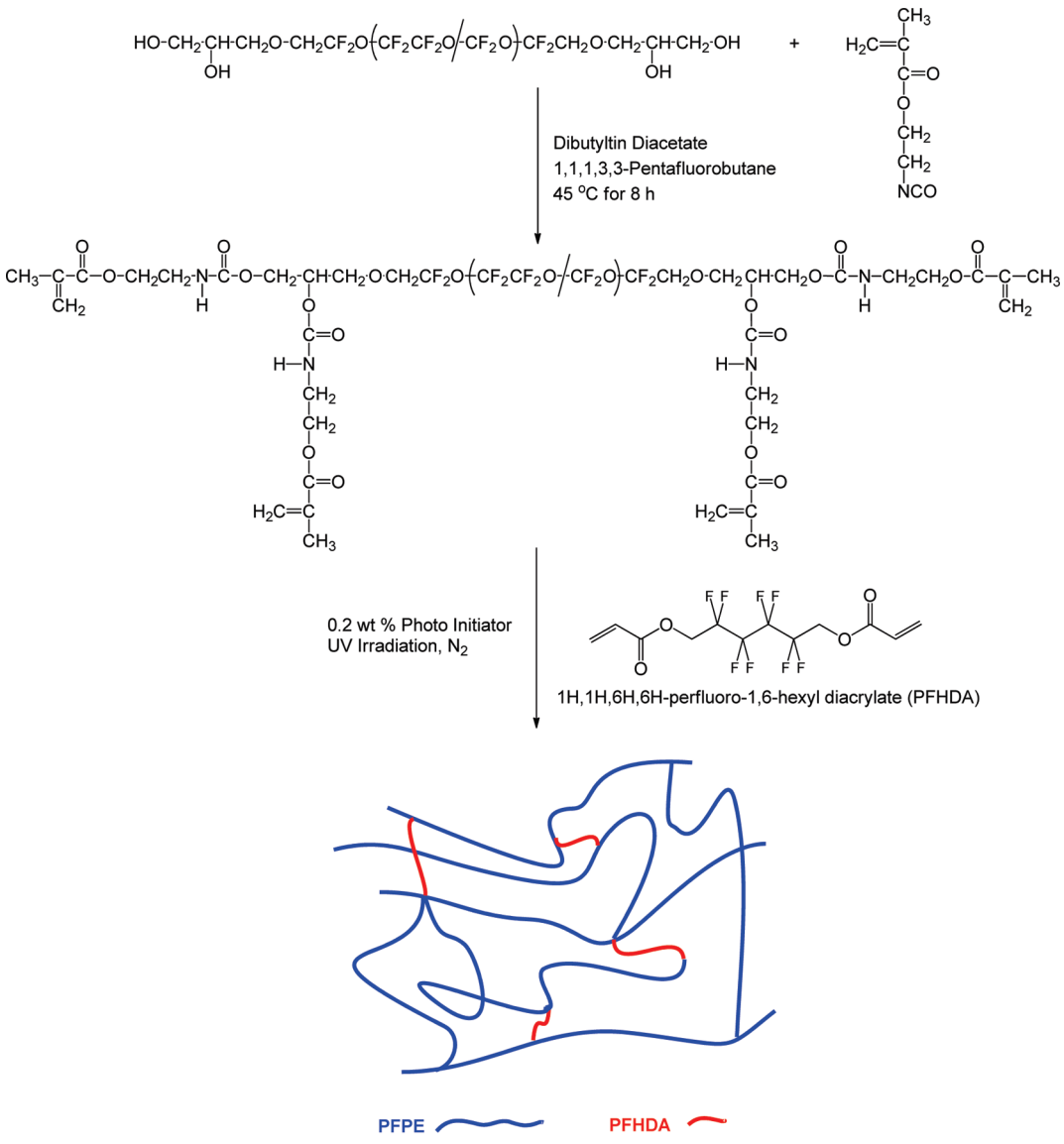

tetrol precursor to yield the PFPETMA macromonomer (Scheme 1). The optically cloudy reaction system became clear ~5 min after the reaction was initiated. With the addition of a photoinitiator, the purified and isolated PFPETMA macromolecule was able to be photochemically cross-linked to form optically transparent films using UV irradiation.

In order to achieve a cross-linked PFPE material with an even higher modulus, a short chain cross-linker was incorporated into the PFPETMA matrix to enhance the degree of cross-linking. The 1*H*,1*H*,6*H*,6*H*-perfluorohexyl diacrylate (PFHDA) was studied as a cross-linker to mix with the PFPETMA macromonomer as it was reasoned the fluorinated nature of PFHDA would help to achieve better miscibility with PFPETMA than many typical hydrocarbon cross-linkers such as poly(ethylene glycol) triacrylate.[32] Additionally, it was also deemed important to use a fluorinated cross-linker to preserve the fluorinated nature of the resulting network materials to minimize the surface tension. It was found that after mixing the liquid mixture using a vortex mixer at room temperature for 2 min an optically clear, homogeneous solution was consistently formed when less than 40 wt % of PFHDA was incorporated, but at 40 wt % and greater, the binary system appeared to be slightly cloudy at room temperature and became progressively cloudier with increasing PFHDA content. Interestingly, the cloudiness of the 40 wt % PFHDA sample disappeared to form an optically clear, homogeneous single-phase solution simply by warming to 36.5 °C. The solution remained optically clear even after cooling to room temperature for days. Similar behavior has been reported by Rábai et al. for a fluorinated binary system.[33] A less compatible binary system was found when the content of PFHDA was further increased to 50 wt %. In this case, mixing of the two components yielded an optically cloudy and thermodynamically unstable emulsion, which readily separated into two phases within 2 h. It is well-known that in some circumstances it is possible for two organic liquids with poor miscibility to reversibly form a homogeneously clear single-phase solution above a certain cloud-point temperature.[34,35] Figure 1 shows the cloud-point temperatures of the PFHDA−PFPETMA liquid binary systems. With a decreasing fraction of the PFPETMA macromonomer in the system, the cloud-point temperature increased from 20 °C at 70 wt % PFPETMA to 80 °C at 20 wt % PFPETMA.

The partial compatibility of PFPETMA with PFHDA was suspected to be a manifestation of the relatively small Flory−Huggins interaction parameter (χ), which is related to the

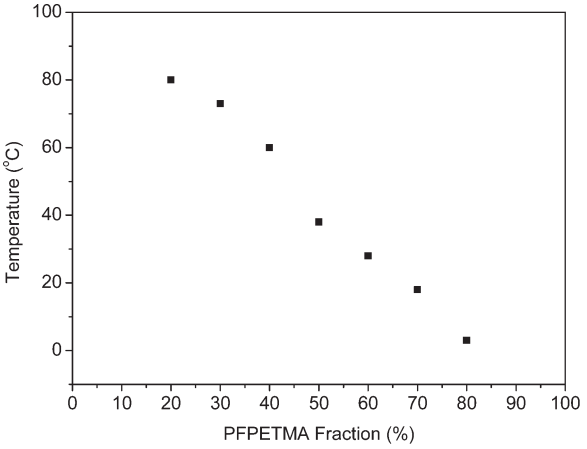

Figure 1. Cloud-point measurements for PFHDA−PFPETMA binary mixtures. The transitions are reversible with heating and cooling variation in cloud point temperature ≈ ±1 °C..

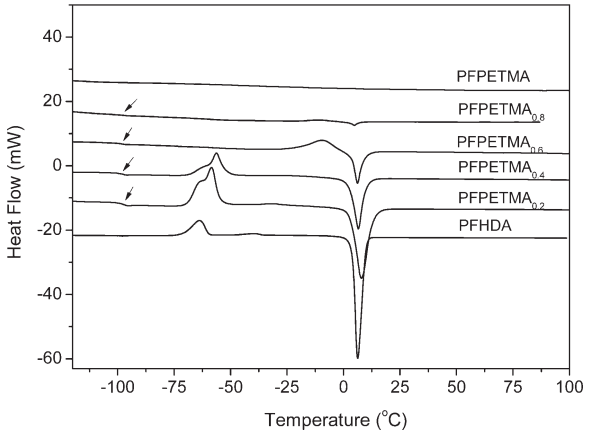

Figure 2. DSC analysis of PFHDA−PFPETMA binary mixtures. The data were shifted on the *y*-axis accordingly for clarity.

Table 1. Thermal Characteristics of PFHDA−PFPETMA Binary Mixtures

	T_g (°C)	T_c (°C)	T_m (°C)
$PFHDA_{0.2}$−$PFPETMA_{0.8}$	−98	−9.5	4.4
$PFHDA_{0.4}$−$PFPETMA_{0.6}$	−100	−12.1	5.6
$PFHDA_{0.6}$−$PFPETMA_{0.4}$	−100	−60.2	6.1
$PFHDA_{0.8}$−$PFPETMA_{0.2}$	−100	−63.6	7.2
PFPETMA	−114	n/a	n/a

solubility parameters of these two components.[36] The end groups identity of the PFPE macromonomers was thought to play a key role on varying the solubility parameter in the studied system. A simple solubility experiment was designed to verify this by first mixing PFHDA with the PFPE oligomer tetrol. We observed that a homogeneous solution could be formed between these two components over all compositions at room temperature. The PFHDA was then mixed with a nonfunctional PFPE oligomer (Fomblin Z03, CF_3−O−(CF_2CF_2O−/−CF_2O)$_n$−CF_3). The oligomer has similar perfluorinated repeat units to the PFPETMA macromonomer but has nonfunctional −CF_3 end groups instead of methacryloxyurethane or hydroxyl end groups. This solubility check indicated that the PFHDA was immiscible with Fomblin Z03 over the entire composition range at room temperature. A dispersion was initially formed by mixing the two components that then quickly separated into two phases. On the basis of these studies, we suggest that the urethane methacryloxy end groups are crucial for enhancing the compatibility of the PFHDA/PFPETMA system, possibly via hydrogen bonds or dispersive interactions between the urethane methacrylate and acrylate end groups.

The glass transition temperatures (T_g) of the PFHDA−PFPETMA binary systems were determined by DSC measurements. As seen in Figure 2, a single T_g was observed for all of the uncured liquid binary systems at around −100 °C, corresponding to the chain mobilization of the fluorocarbon domains. The T_g was slightly lower at −114 °C for the neat liquid PFPETMA macromonomer, which was determined by dynamic differential scanning calorimetry (DDSC) (Table 1).

It is interesting to find a crystallization−melting process involved at low temperatures for all of the liquid binary systems. When 20 wt % of PFHDA was added, a small amount of crystallization was observed at −9.5 °C. This was followed by a melting transition at 4.4 °C upon reheating. The crystallization of PFHDA may be responsible for the cloudiness of this solution at about 3 °C as seen in Figure 1. As the PFHDA content in the system was increased, the crystallization became more pronounced. The crystallization temperature was also found to shift from −9.5 °C for the $PFHDA_{0.2}$−$PFPETMA_{0.8}$ sample to −63.6 °C for the $PFHDA_{0.8}$−$PFPETMA_{0.2}$ sample. Meanwhile, the melting temperatures were only slightly increased from 4.4 to 7.2 °C, respectively. The crystallization−melting process is thought to be involved with the alignment of small PFHDA molecules, not related to the PFPETMA macromonomer, since neither crystallization nor melting was found in the thermogram of the neat PFPETMA sample. Unlike the $PFHDA_{0.2}$−$PFPETMA_{0.8}$ sample, the cloudiness at room temperature of the binary systems with a higher PFHDA content was not associated with the crystallization process because PFHDA crystals completely melted before room temperature was reached. The cloudiness of these samples was therefore mainly attributed to macrophase separation.

By adding 0.2 wt % of HCPK as a photoinitiator, all of the liquid binary samples could be easily photochemically cross-linked to form fluorinated elastomeric films under UV irradiation (Scheme 1). At room temperature, a homogeneous $PFHDA_{0.2}$−$PFPETMA_{0.8}$ solution was cured to yield an optically transparent sample. Because the cloud-point temperature of $PFHDA_{0.4}$−$PFPETMA_{0.6}$ was only 28 °C, the heating generated by the UV irradiation was sufficient to form a clear system before the sample was sufficiently cured. Curing of this homogeneous solution therefore resulted in an optically transparent film. Only the $PFHDA_{0.6}$−$PFPETMA_{0.4}$ and $PFHDA_{0.8}$−$PFPETMA_{0.2}$ systems were cured to yield cloudy samples at room temperature because of the partial incompatibility of these two components. However, optically transparent p($PFHDA_{0.6}$−$PFPETMA_{0.4}$) and p($PFHDA_{0.8}$−$PFPETMA_{0.2}$) samples were obtained when cured at 65 and 85 °C, respectively (Figure 3). The degree of methacrylate group conversion of the cured samples has been monitored by FTIR (see Supporting Information). The absence of the signal due to the C=C stretching of the methacrylic double bonds at 1638 cm^{-1} in the spectrum of the PFPETMA precursor indicates a high monomer conversion.[35] According to rubbery elasticity theory[37] $\upsilon_{E'} = E'/(6RT)$, the cross-link densities ($\upsilon_{E'}$) of the cured binary samples were determined from rubbery plateau data of the storage modulus (E'). The values are listed in Table 2. It clearly indicated that as the content of PFHDA increased from 0 to 80 wt %, the cross-link density of the accordingly cured samples was increased from 55 to 135 mol/L.

No crystallization peak was found for all the cured samples by DSC, but neither was the T_g information on these cross-linked samples detectable by DSC. The T_gs were therefore determined by DMTA through loss factor (tan δ) measurements. The DMTA data are also useful for understanding the morphology and miscibility of the two fluorinated components in this system. Two pronounced relaxation peaks were observed for the neat

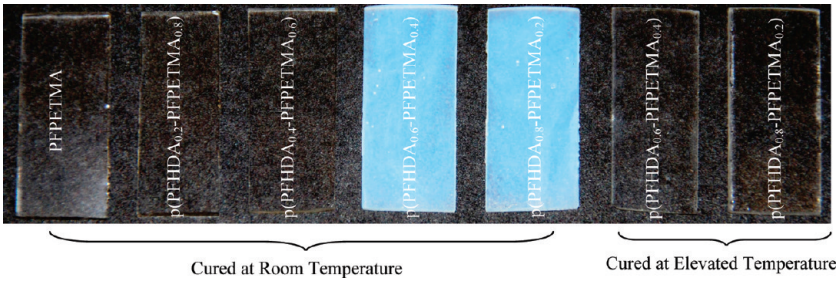

Figure 3. Digital photographs of UV cured p(PFHDA−PFPETMA) binary mixtures.

Table 2. Property Summary of UV-Cured p(PFHDA−PFPETMA) Binary Mixtures

		static contact angle (deg)		surface tension (mN/m)		
	cross-link density ($\upsilon_{E'}$, mol/L)	water	hexadecane	γ_S^d	γ_S^p	γ_S
PFPETMA	55	104.8 ± 1.7	70.5 ± 0.6	12.3	2.3	14.6
p(PFHDA$_{0.2}$−PFPETMA$_{0.8}$)	78	105.5 ± 2.1	70.8 ± 1.0	12.2	2.1	14.3
p(PFHDA$_{0.4}$−PFPETMA$_{0.6}$)	90	103.5 ± 1.3	69.3 ± 0.5	12.6	2.5	15.1
p(PFHDA$_{0.6}$−PFPETMA$_{0.4}$)	123	102.0 ± 2.6	69.0 ± 0.8	12.7	2.9	15.6
p(PFHDA$_{0.8}$−PFPETMA$_{0.2}$)	135	98.3 ± 3.0	65.8 ± 2.2	13.7	3.8	17.5
p(PFHDA)	n/a	96.1 ± 1.8	41.0 ± 2.1	21.2	2.4	23.6

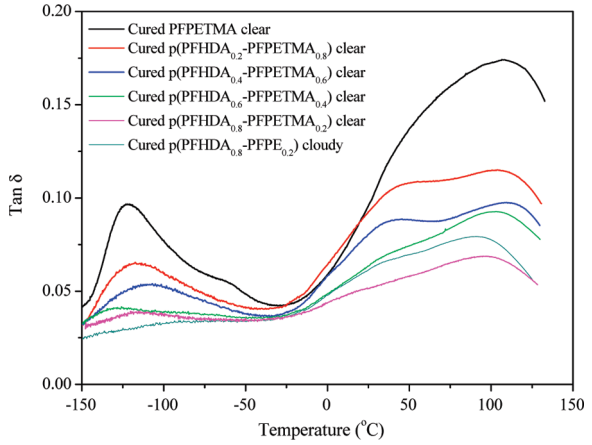

Figure 4. DMTA analysis of UV-cured p(PFHDA−PFPETMA) binary mixtures.

PFPETMA network sample, as seen in Figure 4. The relaxation peak with a maximum at −123 °C was assigned to the fluorocarbon domains from the PFPE segments. Compared to cured dimethacryloxy-functionalized perfluoropolyether (PFPEDMA) materials,[38] the relaxation temperature of the fluorocarbon domains for the cured 2 kg/mol PFPETMA sample was slightly higher than that of the 4 kg/mol PFPEDMA (−130 °C) and lower than the 1 kg/mol PFPEDMA (−80 °C).[25] We hypothesized that the perfluoropolyether segments with longer chains were more flexible in the fluorinated domains. Unlike the PFPEDMA samples, the relaxation peaks from the hydrocarbon domains of the cross-linked methacrylate end groups in the PFPETMA−PHFDA samples appeared to be very broad. For the PFPETMA sample, the relaxation peak ranged from −25 to 140 °C, which indicated a highly microheterogeneous morphology. From the plot, the maximum of the relaxation peak for the hydrocarbon domains from the polymerized methacrylate end groups was determined to be ∼104 °C, which was close to the T_g of poly(methyl methacrylate) (105 °C). A shoulder at about −63 °C was observed for the cured PFPETMA sample. The shoulder was referred to as a β-maximum, generally found in polyurethanes and thought to be related to the hydrogen bonds between contiguous chains.[39] For both the clear p(PFHDA$_{0.2}$−PFPETMA$_{0.8}$) and p(PFHDA$_{0.4}$−PFPETMA$_{0.6}$) samples, a very broad relaxation peak for the copolymerized methacrylate/acrylate domains was observed, which suggests an increased heterogeneity.[40] The β-maximum was not observed for the p(PFHDA−PFPETMA) samples probably because hydrogen bonds associated with the urethane groups of the PFPETMA macromonomer were disrupted by the self-aggregation of the PFHDA. As the fraction of PFHDA increased in the blend matrix, the samples cured at elevated temperatures still appeared to be optically transparent; however, the intensity of the loss factor values (tan δ) of both relaxation peaks for each sample were gradually decreased. The decrease in the loss factor values probably indicated that the chains in both domains (hydrocarbon and fluorocarbon) were less free to mobilize in the blend systems. This could be caused by an increase in the cross-link density through incorporating numerous small PFHDA molecules into the system.[41] Additionally, the DMTA analysis of the cured clear p(PFHDA$_{0.8}$−PFPETMA$_{0.2}$) sample was compared with the cloudy one of the same composition ratio. For the cloudy sample, the relaxation peak for the PFPE segments at ∼−120 °C became undetectable, and the intensity of the relaxation peak in the high temperature region was slightly higher than that of the clear sample. Overall, the difference in the spectra for these two samples is insignificant due to both of them sharing very similar cross-link densities.

The presence of two separate relaxation peaks in the DMTA data indicated that it was a phase-separated system.[42] The clear appearance could only be explained by a phase-separated system with domain sizes smaller than the wavelength of visible light. The domain sizes of the microphase-separated structures formed in the cross-linked PFPETMA−PFHDA blends were investigated by SAXS. Figure 5 shows the one-dimensional scattering profiles from azimuthal integration of 2-dimensional patterns. The data were plotted as scattering intensity vs the principal scattering vector $q = [4\pi \sin(\theta)/\lambda]$ (2θ = scattering angle; λ = wavelength). The cross-linked PFPETMA sample exhibited a relatively broad peak with a maximum at $q \sim 1.2$ nm^{-1} corresponding to a domain size (d) of 5.2 nm according to $d = 2\pi/q$. A very sharp peak appeared embedded in the broad signal with a maximum at $q \sim 1.2$ nm^{-1} ($d = 5$ nm). At this time, we cannot confidently assign this signal to any particular structural feature. The broad peak indicated a microphase-separated structure lacking long-range order. The relatively small length scale was consistent with domains likely consisting of polymerized

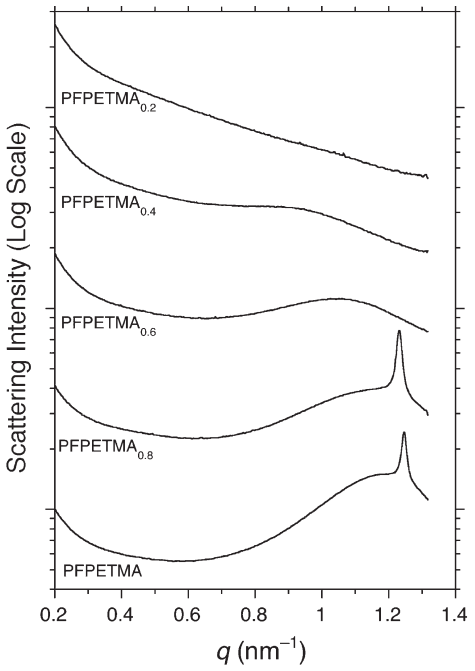

Figure 5. SAXS analysis of the UV-cured p(PFHDA−PFPETMA) binary mixtures.

aggregates of methacrylate end groups separated from the perfluoropolyether midsegments. The maxima of the principal scattering reflections monotonically decreased with increasing PFHDA content, consistent with increasing domain sizes as PFHDA aggregates were preferentially polymerized into separate domains containing the aliphatic methacrylate chain ends. Samples p($PFHDA_{0.4}$−$PFPETMA_{0.6}$), p($PFHDA_{0.6}$−$PFPETMA_{0.4}$), and p($PFHDA_{0.8}$−$PFPETMA_{0.2}$) have d equal to 5.9, 7.2, and 12.5 nm, respectively. The relatively large breadth of the scattering peaks suggested a broad distribution of domain sizes in these poorly ordered systems, which was consistent with the structures observed by AFM (see Figure 6). We posit that the scattering intensity decreases with increasing PFHDA content due to the decreasing electron density contrast between the fluorinated PFHDA and perfluoropolyether segments in the PFPETMA. However, the optical clarity of the samples combined with the scattering suggested that all the samples were microphase separated after cross-linking.

The bulk morphologies of the cured p(PFHDA−PFPETMA) samples were investigated by AFM. Tapping mode phase contrast images were taken on the cross sections of these samples. To minimize the effect of roughness on the phase images of the studied samples, flat cross sections were obtained using an ultramicrotome, resulting in a typical surface rms ≈2 − 3 nm (rms roughness values for the neat PFPETMA sample were < 1 nm). As seen in Figure 6a, the cross section of the neat PFPETMA sample seems highly disordered. The small domains of 3−5 nm from the polymerized methacrylate end groups were randomly distributed in the continuous PFPE matrix. When 20 wt % of PFHDA was added into the PFPETMA, the domain size slightly increased to 6−10 nm (Figure 6b). Further increasing the content of PFHDA to 40 wt % resulted in a more heterogeneous cross section and also increased the domain size from less than 10 nm to 10−30 nm as shown in Figure 6c. The increased domain size was a result of the self-aggregation of PFHDA beginning to dominate the interactions of PFHDA with the methacrylate end groups of the PFPETMA chains. When PFHDA became the major component of the blend system, some domains as large as 50 nm formed (see Figure 6d for the cured p($PFHDA_{0.6}$−$PFPETMA_{0.4}$) clear sample). The difference in reactivity between the acrylate and methacrylate functional groups should also be taken into consideration in the study of the enhanced phase separation of cross-linked samples. Because of the greater reactivity of the acrylate groups, a microgel structure with a higher cross-link density localized around a center of initiation was easier to form, which resulted in a higher degree of phase separation in cross-linked samples with increasing PFHDA content.

As the PFHDA content was increased to 60 wt %, the number of the isolated domains from the copolymerized methacrylate/acrylate end groups was increased, and the boundary between these isolated domains and the continuous PFPE matrix appeared sharper compared to that in Figure 6c for the p($PFHDA_{0.6}$−$PFPETMA_{0.4}$) clear sample. These changes in the morphology presumably indicated a decreased compatibility of the two components in the copolymerized system. When the PFHDA content was increased to 80 wt %, some isolated domains were observed with a domain size of 30−50 nm and many domains began to aggregate with each other to form a striplike morphology of 10−30 nm in thickness and 50−200 nm in length as shown in Figure 6e. In this case, a cocontinuous biphasic morphology began to form. In contrast, the neat p(PFHDA) sample gave a very homogeneous cross section without any noticeable domains observed (Figure 6f). The AFM phase contrast images showed a transition in the bulk morphologies of the materials as the PFHDA content was increased, thus indicating that as more PFHDA was added, a less miscible system was obtained.

Additionally, the AFM phase contrast images were compared for two pairs of clear and cloudy samples in the composition ratios of 60 and 80 wt %. We observed that the morphologies of the two cloudy samples in Figure 6g,h were very different from those of the corresponding clear samples in Figure 6d,e. The cloudy samples possessed more heterogeneous cross sections with some large domains of several hundred nanometers in size, resulting in the cloudy appearance of the samples. In contrast, the optically transparent samples were only microphase separated and thus did not scatter visible light.

Compared to the previously studied PFPE elastomer materials cross-linked from difunctional linear macromonomers, the cross-linked tetramethacryloxy-modified PFPE material with $f = 8$ possesses a higher degree of cross-linking. The modulus of PFPETMA (M_n = 2 kg/mol) was measured by the stress−strain curve to be 155 ± 6 MPa as seen in Figure 7. The "turnover" in data plots only indicates the break point at elongation. This was much higher than that of the dimethacryloxy-functionalized perfluoropolyether (PFPEDMA) samples (7 MPa for M_n = 4 kg/mol and 90 MPa for M_n = 1 kg/mol) because of the enhanced cross-link density in the PFPETMA network induced by both chemical cross-linking and physical cross-linking (hydrogen bonds).[38] It is expected that the Young's modulus of the blend system can be further increased by copolymerizing with the short chain cross-linker PFHDA. When 20 wt % of PFHDA was added, the modulus was increased to 267 ± 11 MPa, and when 80 wt % of PFHDA was added, a very rigid material with a modulus of 458 ± 47 MPa was achieved.

In order to enhance the modulus while also preserving the low surface tension of the PFPE fluorinated elastomer, it was anticipated to be best to use a low molar mass fluorinated cross-linker such as PFHDA as a comonomer with the PFPE macromonomer. In this way the cross-link density could be increased, resulting in a higher modulus, while the fluorinated nature of the network was preserved which resulted in a minimal surface tension for the material. Surface tensions of the p(PFHDA−PFPETMA) materials were calculated based on the Owens−Wendt−Kaelble method (OWK):[43,44]

$$\gamma_L = 2\frac{(\gamma_S^d\gamma_L^d)^{1/2} + (\gamma_S^p\gamma_L^p)^{1/2}}{1+\cos\theta} \quad (1)$$

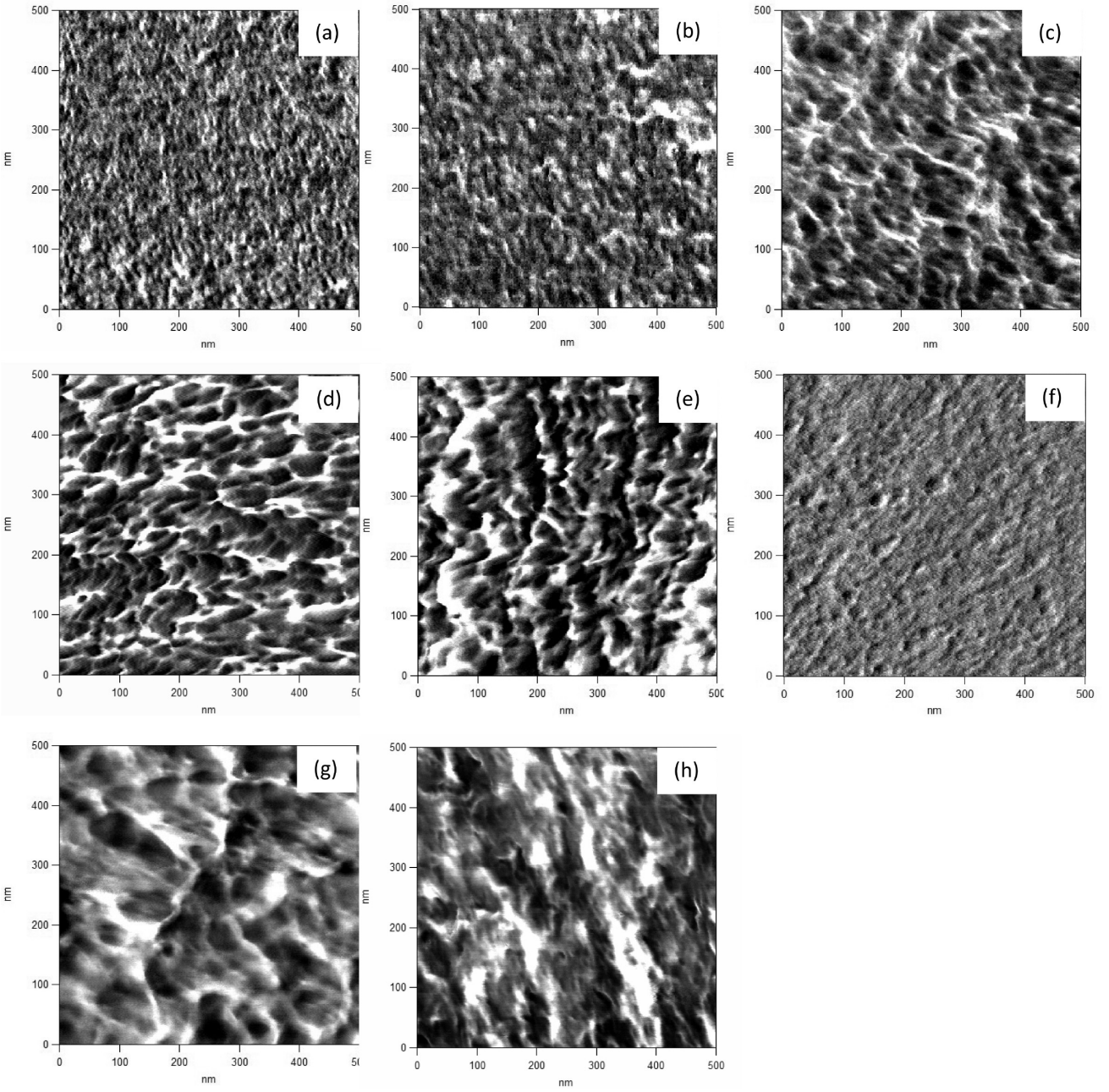

Figure 6. AFM phase contrast images in tapping mode on cross sections of UV-cured p(PFHDA−PFPETMA) binary mixtures: (a) PFPETMA, (b) clear p($PFHDA_{0.2}$−$PFPETMA_{0.8}$), (c) clear p($PFHDA_{0.4}$−$PFPETMA_{0.6}$), (d) clear p($PFHDA_{0.6}$−$PFPETMA_{0.4}$), (e) clear p($PFHDA_{0.8}$−$PFPETMA_{0.2}$), (f) p(PFHDA), (g) cloudy p($PFHDA_{0.6}$−$PFPETMA_{0.4}$), and (h) cloudy p($PFHDA_{0.8}$−$PFPETMA_{0.2}$).

where θ is the static contact angle, γ_L is the surface tension of a probe liquid, and γ_L^d and γ_L^p are the dispersive component and the polar component of the liquid surface tension, respectively. By measuring the contact angles of two different probe liquids (one polar and one nonpolar) on each surface, the overall solid surface tension could be calculated based on the equation. The OWK method can distinguish the contributions of dispersive and polar components to the overall surface tension. The static contact angles of water and *n*-hexadecane were measured at air interfaces of cross-linked samples cured at room temperature. The resulting surface tensions were calculated and are summarized in Table 2. The surface tension of the neat PFPETMA sample was found to be 14.6 mN/m. When incorporating 20 wt % of PFHDA into the cross-linked PFPE system, the surface tension remained consistently low (14.3 mN/m). Further increasing the PFHDA content slightly decreased both the water and hexadecane contact angles, resulting in slightly increased contributions of dispersive and polar components to the overall surface tensions. Then, when 80 wt % of PFHDA was incorporated, the overall surface tension increased to 17.5 mN/m. Furthermore, the surface tension of a homogeneous p(PFHDA) sample was measured and found to be 23.6 mN/m. A large contribution of the dispersive component was observed and resulted in a relatively higher overall surface tension for this material. Compared to other fluorinated samples, the increased dispersive component was mainly attributed to the less hydrophobic nature of the PFHDA cross-linker. Along with the lower surface tension, the greater durability of these PFPE materials would be an advantage over existing technologies since one of limiting factors of the performance of soft fouling-release materials, such as silicone, is that their low modulus makes them prone to physical damage in long-term ocean trials.

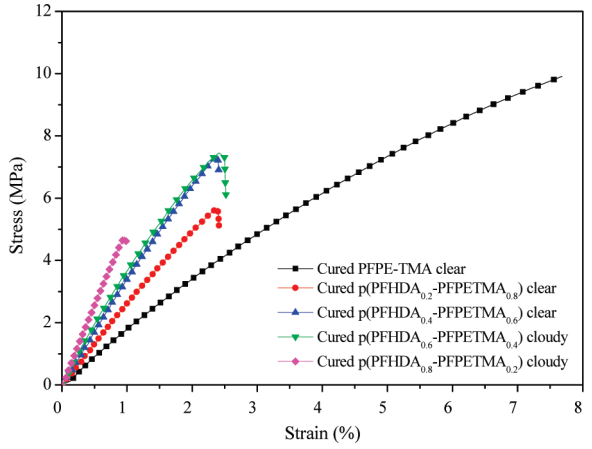

Figure 7. Tensile testing of UV-cured p(PFHDA−PFPETMA) binary mixtures.

Conclusions

In this work, we synthesized tetramethacryloxy-modified perfluoropolyethers that can be photochemically cross-linked by UV irradiation in one step to yield a fluorinated network with improved modulus. With hydrogen bonds and dispersive interactions between the urethane ether methacrylate and fluorinated acrylate groups, PFHDA showed partial miscibility with the PFPETMA macromonomer. When <40 wt % of PFHDA was mixed with the PFPETMA macromonomer, a homogeneous clear solution could be formed at room temperature. However, when the PFHDA became the major component of the liquid binary system, the self-aggregation of the PFHDA began to dominate the intermolecular interactions between these two components, resulting in an immiscible system. The cloud-point temperature data indicated that as the content of the PFHDA in the binary system was increased, the miscibility between the two components was decreased, and therefore a homogeneous clear solution was only able to be achieved at elevated temperatures. Because of the partial immiscibility of these two components, optically transparent materials with PFHDA content of less than 40 wt % can be obtained via UV curing at room temperature. However, optically transparent samples with PFHDA content larger than 40 wt % can be achieved by controlling the cure temperature above the corresponding cloud-point temperature of the system. The DMTA spectra indicated that the partial immiscibility of the two components resulted microphase separation even in the cured clear samples. AFM contrast images further confirmed the microphase-separated morphology of these optically transparent materials.

The Young's moduli of these materials (155−458 MPa) were much higher than those reported for PDMS and other fluorinated elastomer materials. Along with the low surface tensions (14.3−17.5 mN/m), these materials should be suitable for enhanced for fouling-release coating applications. Studies on these two-component systems will help to fundamentally understand the miscibility issues associated with fluorinated monomers and lead to an optimized design for more compatible fluorinated materials with better durability.

Acknowledgment. This research is partially supported by the Office of Naval Research under Awards #N00014-02-1-0185 (J.M.D.), the STC program of National Science Foundation, Liquidia Technologies, and the William R. Kenan, Jr. Distinguished Professorship of the University of North Carolina at Chapel Hill. The portion of this work performed at the Advanced Photon Source (APS) at Sector 5 is supported by E. I. DuPont de Nemours and Co., The Dow Chemical Company, and the State of Illinois. Use of the APS was supported by the U.S. Department of Energy, Office of Science, Office of Basic Energy Sciences, under Contract DE-AC02-06CH11357. Partial support from the National Science Foundation (DMR-0605880) is also acknowledged. We thank Dr. Yapei Wang for preparing samples for SAXS examination and also thank Dr. Douglas Betts for helpful discussions.

Supporting Information Available: FTIR spectra of the PFPETME precursor and cured blends. This material is available free of charge via the Internet at http://pubs.acs.org.

References and Notes

(1) Walter, D. M.; Alfred, B. S. *J. Biomed. Mater. Res.* **1972**, *6*, 193–199.
(2) Choi, K. M.; Rogers, J. A. *Mater. Res. Soc. Symp. Proc.* **2003**, *788*, 491.
(3) Rolland, J. P.; Hagberg, E. C.; Denison, G. M.; Carter, K. R.; DeSimone, J. M. *Angew. Chem., Int. Ed.* **2004**, *43*, 5796–5799.
(4) Truong, T. T.; Lin, R.; Jeon, S.; Lee, H. H.; Maria, J.; Gaur, A.; Hua, F.; Meinel, I.; Rogers, J. A. *Langmuir* **2007**, *23*, 2898–2905.
(5) Wiles, K. B.; Wiles, N. S.; Herlihy, K. P.; Maynor, B. W.; Rolland, P., J.; DeSimone, J. M. *Proc. SPIE* **2006**, *6151*, 61513F1–61513F9.
(6) Rolland, J. P.; VanDam, R. M.; Schorzman, D. A.; Quake, S. R.; DeSimone, J. M. *J. Am. Chem. Soc.* **2004**, *126*, 2322–2323.
(7) Brady, R. F.; Singer, I. L. *Biofouling* **2000**, *15*, 73.
(8) Baier, R. E.; Loeb, G. I.; Wallace, G. A. *Fed. Proc.* **1971**, *30*, 1523–1528.
(9) Singer, I. L.; Kohl, J. G.; Patterson, M. *Biofouling* **2000**, *15*, 301.
(10) Finlay, J. A.; Callow, M. E.; Ista, L. K.; Lopez, G. P.; Callow, J. A. *Integr. Comput. Biol.* **2002**, *42*, 1116.
(11) Ista, L. K.; Callow, M. E.; Finlay, J. A.; Coleman, S. E.; Nolasco, A. C.; Simons, R. H.; Callow, J. A.; Lopez, G. P. *Appl. Environ. Microbiol.* **2004**, *70*, 4151.
(12) Callow, J. A.; Callow, M. E.; Ista, L. K.; Lopez, G.; Chaudhury, M. K. *J. R. Soc. Interface* **2005**, *2*, 319.
(13) Walker, G. C.; Sun, Y.; Guo, S.; Finlay, J. A.; Callow, M. E.; Callow, J. A. *J. Adhes.* **2005**, *81*, 1101–1118.
(14) Chaudhury, M. K.; Finlay, J. A.; Chung, J. Y.; Callow, M. E.; Callow, J. A. *Biofouling* **2005**, *21*, 41.
(15) Marabotti, I.; Morelli, A.; Orsini, L. M.; Martinelli, E.; Galli, G.; Chiellini, E.; Lien, E. M.; Pettitt, M. E.; Callow, M. E.; Callow, J. A.; Conlan, S. L.; Mutton, R. J.; Clare, A. S.; Kocijan, A.; Donik, C.; Jenko, M. *Biofouling* **2009**, *25*, 481–493.
(16) Brady, R. F. *J. Coat. Technol. Res.* **2000**, *72*, 46.
(17) Pike, J. K.; Ho, T.; Wynne, K. J. *Chem. Mater.* **1996**, *8*, 856.
(18) Kendall, K. *J. Phys. D: Appl. Phys.* **1971**, *4*, 1186.
(19) Efimenko, K.; Finlay, J.; Callow, M. E.; Callow, J. A.; Genzer, J. *ACS Appl. Mater. Interfaces* **2009**, *1*, 1031–1040.
(20) Hoipkemeier-Wilson, L.; Schumacher, J. F.; Carman, M. L.; Gibson, A. L.; Feinberg, A. W.; Callow, M. E.; Finlay, J. A.; Callow, J. A.; Brennan, A. B. *Biofouling* **2004**, *20*, 53–63.
(21) Chisholm, B. J.; Stafslien, S. J.; Christianson, D. A.; Gallagher-Lein, C.; Daniels, J. W.; Rafferty, C.; Wal, L. V.; Webster, D. C. *Appl. Surf. Sci.* **2007**, *254*, 692–698.
(22) Yarbrough, C.; Rolland, J. P.; DeSimone, J. M.; Callow, M. E.; Finlay, J. A.; Callow, J. A. *Macromolecules* **2006**, *39*, 2521–2528.
(23) Gudipati, C. S.; Finlay, J. A.; Callow, J. A.; Callow, M. E.; Wooley, K. L. *Langmuir* **2005**, *21*, 3044.
(24) Scheirs, J. *Modern Fluoropolymers*; John Wiley & Sons, Ltd.: New York, 1997.
(25) Hu, Z.; Finlay, J.; Chen, L.; Betts, D.; Hillmyer, M.; Callow, M.; Callow, J.; DeSimone, J. M. *Macromolecules* **2009**, *42*, 6999–7007.
(26) Provder, T.; Malliprakash, S.; Amin, S. H.; Majid, A.; Texter, J. *Macromol. Symp.* **2006**, *242*, 279–289.
(27) Mirabedinia, S. M.; Mohsenib, M.; PazokiFarda, S.; Esfandeh, M. *Colloids Surf., A* **2008**, *317*, 80–86.
(28) Xu, J.; Bartels, J. W.; Bohnsack, D. A.; Tseng, T.-C.; Mackay, M. E.; Wooley, K. L. *Adv. Funct. Mater.* **2008**, *18*, 2733.
(29) Hanson, D. E. *Polymer* **2004**, *45*, 1055–1062.
(30) Chen, Z.; Chisholm, B.; Kim, J.; Stafslien, S.; Wagner, R.; Patel, S.; Daniels, J.; Vander, L.; Li, W. J.; Ward, K.; Callow, M.; Thompson, S.; Siripirom, C. *Polym. Int.* **2008**, *57*, 879–886.

(31) Ekin, A.; Webster, D. C.; Daniels, J. W.; Stafslien, S. J.; Cassé, F.; Callow, J. A.; Callow, M. E. *J. Coat. Technol. Res.* **2007**, *4*, 435.
(32) Elbert, D. L.; Pratt, A. B.; Lutolf, M. P.; Halstenberg, S.; Hubbell, J. A. *J. Controlled Release* **2001**, *76*, 11–25.
(33) Horváth, I. T.; Rábai, J. *Science* **1994**, *266*, 72–75.
(34) Watanabe, H. In *Solution Behavior of Surfactants*; Plenum Press: New York, 1982; pp 1305−1313.
(35) Bruns, N.; Tiller, J. C. *Macromolecules* **2006**, *39*, 4386–4394.
(36) Rubinstein, M.; Colby, R. H. *Polymer Physics*; Oxford University Press: New York, 2003.
(37) Flory, P. J. *Principles of Polymer Chemistry*; Cornell University Press: Ithaca, NY, 1990.
(38) Hu, Z.; Chen, L.; Betts, D. E.; Pandya, A.; Hillmyer, M. A.; DeSimone, J. M. *J. Am. Chem. Soc.* **2008**, *130*, 14244–14252.
(39) McCrum, N. G.; Read, B. E.; Williams, G. *Inelastic and Dielectric Effects in Polymeric Solids*; Dover: New York, 1991.
(40) Young, J. S.; Kannurpatti, A. R.; Bowman, C. N. *Macromol. Chem. Phys.* **1998**, *199*, 1043–1049.
(41) Hourston, D. J.; Schäfer, F.-U.; Gradwell, M. H. S.; Song, M. *Polymer* **1998**, *39*, 5609–5617.
(42) Yao, S. In *Advances in Interpenetrating Polymer Networks*; Klempner, D., Frisch, K. C., Eds.; Technomic: Lancaster, 1994; Vol. *IV*.
(43) Owens, D. K.; Wendt, R. C. *J. Appl. Polym. Sci.* **1969**, *13*, 1741–1747.
(44) Kaelble, D. H. *J. Adhes.* **1970**, *2*, 66–81.